Proceedings of the
International Conference on Mechanical Engineering 2005
(ICME2005) 28- 30 December 2005, Dhaka, Bangladesh

ICME05-FL-17

A NUMERICAL STUDY OF SOOT FORMATION IN A LAMINAR METHANE-AIR DIFFUSION FLAME UNDER EARLY TRANSIENT CONDITION

B. K. Mandal[1], A. Datta[2] and A. Sarkar[3]

[1]Department of Mechanical Engineering, B.E. College (Deemed University), Howrah 711109, INDIA
[2]Department of Power Engineering, Jadavpur University, Salt Lake Campus, Kolkata 700098, INDIA
[3]Department of Mechanical Engineering, Jadavpur University, Kolkata 700032, INDIA

ABSTRACT

The soot formation in a laminar methane/air diffusion flame under early transient condition has been numerically investigated. A two equations model for soot volume fraction and number density in laminar diffusion flame has been considered. Nucleation, surface growth, coagulation and oxidation effects are taken into account in the formation of the model equations. The computed results show that following ignition the soot is formed in the flame when the flame front temperature exceeds a certain value (about 1300 K). Initially, when the oxidization of the soot is not significant, some of the soot particles of small diameter escape out of the solution domain. However, under the steady condition, the soot which is formed within the flame zone, gets totally oxidized beyond the flame and the product gas escapes with no soot.

Keywords: Diffusion flame, Soot volume fraction , Transient, Finite difference.

1. INTRODUCTION

The formation and emission of pollutant during combustion has become a matter of increasing concern over the last two decades. Hence, the research in the field of combustion engineering has shifted its focus from improving the combustion efficiency to reducing combustion generated pollutant emission. Soot is an atmospheric pollutant formed in hydrocarbon combustion, which causes respiratory illness and increases mortality. Soot in flame results from incomplete combustion of hydrocarbons in the reducing atmosphere. According to Haynes and Wagner [1], pyrolysis of hydrocarbon fuel molecules break them up into smaller hydrocarbons and finally to acetylene. The initial step of the formation of soot is the production of aromatic species from the aliphatic hydrocarbons, e.g. acetylene. The aromatic species grow by combining with other aromatic and alkyl species to form large polyaromatic hydrocarbons (PAH). Continued growth of PAH molecules eventually lead to the smallest identifiable soot particles. On the other hand, soot contributes significantly to the radiative heat transfer from the flame and plays a major role in furnace heat transfer. Therefore, better understanding and control of soot forming processes in hydrocarbon combustion are required.

Diesel engines where the fuel and air remain initially non-premixed are a prime source of soot in the atmosphere. The combustion process in the diesel engine is transient, where the flame first appears, then propagates and finally extinguishes with the progress of the expansion process. In co-flowing gas burners having diffusion flames, during ignition and initial lighting up of the flame, a transient situation arises when the combustion phenomenon differs from the subsequent steady situation.

A great number of studies have been undertaken for further understanding of the mechanisms responsible for soot formation under a variety of different combustion conditions. Wey *et al.*[2], Santoro *et al.*[3], Smooke *et al.*[4], Lee *et al.*[5] and Xu *et al.*[6] performed experiments in laminar diffusion flames using various hydrocarbon fuels for the determination of soot. Wey *et al.*[2] found that the soot volume fraction and aggregate diameters increased with the height above the burner, while the opposite was the case with number densities. Santoro *et al.*[3] experimented with various fuels and observed that the increase in soot formation is primarily due to an increase in the residence time in the annular region of the diffusion flame. Smooke *et al.*[4] measured the soot volume fraction as well as the concentrations of fuel (methane), acetylene and benzene within the flame zone of a co-flowing laminar jet diffusion flame. Lee *et al.*[5] observed that the rate of soot inception became stronger with the oxygen enriched oxidizer stream. Xu *et al.*[6] studied the soot surface growth and oxidation in laminar hydrocarbon-air diffusion flames at atmospheric pressure with several fuels. It was found that the fuel type did not affect the soot surface oxidation rates.

For numerical computation, different soot models were proposed by Smith [7], Gore and Faeth [8], Kennedy *et al.*[9], Syed *et al.*[10], Moss *et al.*[11] and Said *et al.*[12]. Soot oxidation plays an important role in controlling emission level. Different soot oxidation models proposed by Lee *et al.*[13], Nagle and Strickland-Constable [14] and Najjar and Goodger [15] are in vogue.

The works conducted in laminar diffusion flames for the prediction of formation and distribution of soot used steady flames under different operating conditions and fuels. No work is available in the literature where such studies have been conducted in a transient flame following ignition. There are applications, e.g. in diesel engines or during light-up of a burner flame, when the flame is not steady. Therefore, it would be interesting to investigate the development of soot volume fraction and average size in a transient and moving flame.

2. THEORETICAL FORMULATION

The combustion is modeled as an axi-symmetric confined laminar diffusion flame with fuel (methane) admitted as a central jet and air as a co-flowing annular jet. The diameters of the inner fuel tube and outer tube are 12.7 mm and 50.4 mm respectively and the length of the computational domain is 0.3 m. The combustion process is simulated with a detailed numerical model, solving the governing equations for a laminar, axi-symmetric, reacting flow with appropriate boundary conditions. The flow is vertical through the reaction space and the gravity effect is included in the momentum equation. A variable property formulation has been made for the transport and thermodynamic properties [16]. A simplified two steps reaction chemistry has been adopted for methane combustion and radiation heat transfer from the flame is neglected. The conservation equations for mass, radial momentum, axial momentum, species concentrations and energy in cylindrical co-ordinates for axisymmetric geometry are solved to get the velocity, temperature and species concentration distributions in the computational domain [17].

For the soot model, the soot volume fraction (f_v) and number density (n) are considered to be the important variables. Nucleation, surface growth, coagulation and oxidation effects are taken into account in the formation of the model equations following Syed *et al.*[10] and Moss *et al.*[11]. The model proposed by Lee *et al* .[13] is used for soot oxidation. The conservation equations are formed for soot mass concentration ($\rho_s f_v$) and number density (as n/N_o) and the respective generation terms for the conservation equations are as follows:

$$\frac{d}{dt}\left(\rho_S f_V\right) = \gamma \left(\rho_S f_V\right)^{2/3} n^{1/3} + \delta - \left(\frac{36\pi}{\rho_S^2}\right)^{1/3} \left(n \rho_S^2 f_V^2\right)^{1/3} \omega_{ox} \quad (1)$$

$$\frac{d}{dt}\left(\frac{n}{N_o}\right) = \alpha - \beta\left(\frac{n}{N_o}\right)^2 \quad (2)$$

The soot model constants α, β, γ and δ are calculated following Syed *et al.* [10] and the coagulation term (second term on R.H.S. in Eq. 2) is derived from the Smolushowski equation for coagulation of liquid colloids [18]. Conservation equations for the soot mass concentration ($\rho_s f_v$) and number density (n/N_o), in general, can be expressed as,

$$\frac{\partial \varphi}{\partial t} + \frac{1}{r}\frac{\partial}{\partial r}\left(r\, v_r\, \varphi\right) + \frac{\partial}{\partial z}\left(\rho\, v_z\, \varphi\right) = \frac{1}{r}\frac{\partial}{\partial r}\left(r\, V_{t_r}\, \varphi\right) + \frac{\partial}{\partial z}\left(V_{t_z}\, \varphi\right) + \dot{S}_\varphi \quad (3)$$

The thermophoretic velocity vector (V_t) in the above equation is calculated following Santoro *et al.*[3].

3. NUMERICAL METHOD

The gas phase conservation equations of continuity, momentum, energy and species concentrations along with the conservation equations of soot mass concentration and number density are solved simultaneously, with their appropriate boundary conditions, by an explicit finite difference computing technique. The variables are defined following a staggered grid arrangement.

Boundary conditions at the inlet are given separately for the fuel stream at the central jet and the air stream at the annular co-flow. The temperature of the fuel stream at the entry is considered to be 300 K. No soot enters with the flow through the inlet plane. Considering the length of the computational domain to be 0.3 m, the fully developed boundary conditions for the variables are considered at the outlet. In case of reverse flow at the outlet plane, which occurs in the case of buoyant flame, the stream coming in from the outside is considered to be atmospheric air. Axi-symmetric condition is considered at the central axis, while at the wall a no-slip, adiabatic and impermeable boundary condition is adopted. The ignition is simulated by increasing the temperature of a few cells a little above the burner tip and at the interface of the two jets.

The incremental time-step has been chosen in such a way that pure advection should not convey a fluid element past a cell and also the fluxes should not diffuse more than one cell in a time step.

A variable size adaptive grid system is considered with higher concentration of nodes near the axis, where larger variations of the variables are expected. A numerical mesh with 85×41 grid nodes is finally adopted after a rigorous grid independence test

4. RESULTS AND DISCUSSION

The numerical code for the reacting flow is validated by comparing the predictions against experiments

conducted by Mitchell *et al.*[19]. Radial distributions of temperature and major product species (CO_2 and H_2O) concentrations at a height of 12 mm above the burner rim are compared and a good agreement is obtained. The soot model employed in the present work is calibrated against the more recent experimental results of Smooke *et al.*[4] for the same burner configuration and input conditions as shown in figure 1.

The steady velocity and temperature distributions along with the flame front surface have been presented in Fig. 2. The details of the velocity and temperature fields development starting from the point of ignition to the steady state have been discussed elsewhere [17].

Figures 3a-f show the distributions of soot volume fractions along with the flame contour at different times after ignition. It is seen in figure 3a that though a thin flame is established 0.05 s after the ignition is given, the soot volume fraction is very low. With the passage of time, the soot formation process accelerates with the increase in the rate of nucleation and growth. The increase in temperature plays a major role in achieving this.

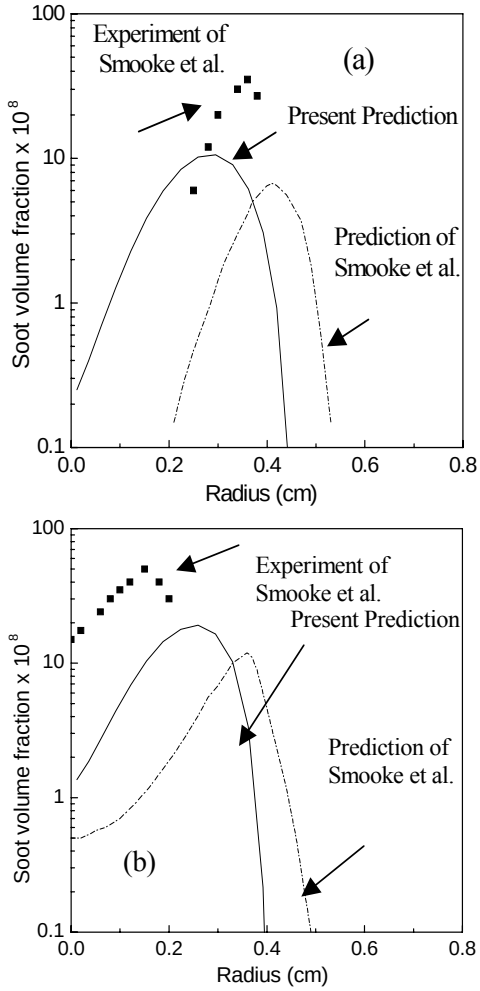

Fig 1. Radial distribution of soot volume fraction in diffusion flame at non-dimensional axial heights (a) $Z/H_F = 0.5$, (b) $Z/H_F = 0.69$: Comparison of the present prediction against Smooke *et al.*[3].

At 0.1 s, the maximum soot volume fraction reaches a value of 60×10^{-8}. A high contour value of 40×10^{-8} is observed inside the flame. The high soot concentration zone is observed inside the flame surface because of the high fuel concentration there. Beyond the flame, the soot particles are oxidized due to the presence of oxygen at high temperature. The maximum soot volume fraction at 0.15 s after ignition is 120×10^{-8}, which is much more than the peak values of the earlier time. A high soot concentration contour of 60×10^{-8} is shown in Fig. 3c. The region over which the soot particles are found to exist in good proportion has also increased along with the increase in the volume fraction, indicating an increase in the overall quantity of soot particles formed in the flame. Subsequent to this time, the peak soot concentration falls and at 0.2 s the highest soot volume fraction is 67×10^{-8} (Fig. 3d). The higher soot formation during the earlier time was due to the accumulated fuel in the chamber that remained unburnt due to the absence of the flame front surface. Once the accumulated fuel is burnt, conditions tend towards the steady state and maximum soot volume fraction comes down. The soot distributions at 0.4 s and 0.8 s after ignition are similar (figures 3e and 3f). The flame and hence the soot formation reaches its steady state before 0.4 s, and the transience in the domain continues till 0.8 s only because of adjustments in the post flame region.

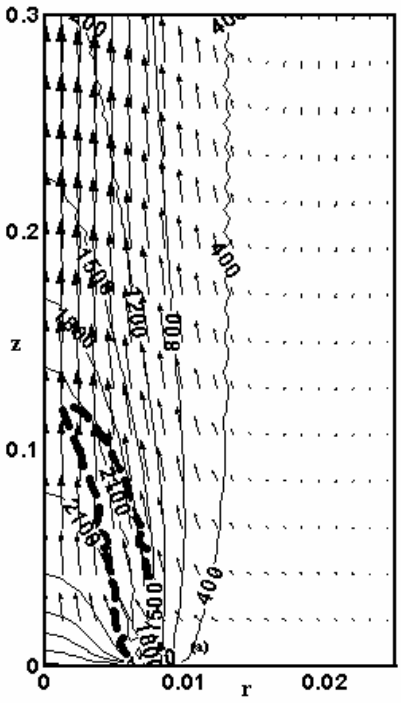

Fig 2. Flame front surface (thick dashed line), temperature (in K) field and velocity field for the steady diffusion flame.

Figures 4a and 4b show the variation of the total soot volume and cumulative soot particle number within the solution domain with time measured from the point of ignition. It is observed from the figures that both the soot volume and soot particle number first increase to reach a

peak and subsequently decrease and finally reach a steady value. However, the time at which the two quantities reach their peak values are different. Accordingly, five time zones can be identified:

i) 0 to 0.15 s – when both the soot volume and particle number increase with time.
ii) 0.15 to 0.225 s – when the soot volume decreases but the particle number increases.
iii) 0.225 to 0.275 s – when the soot volume remains constant but particle number still increases.
iv) 0.275 to 0.6 s – when soot volume remains constant but particle number decreases
v) Beyond 0.6 s – when both soot volume and particle number remain constant.

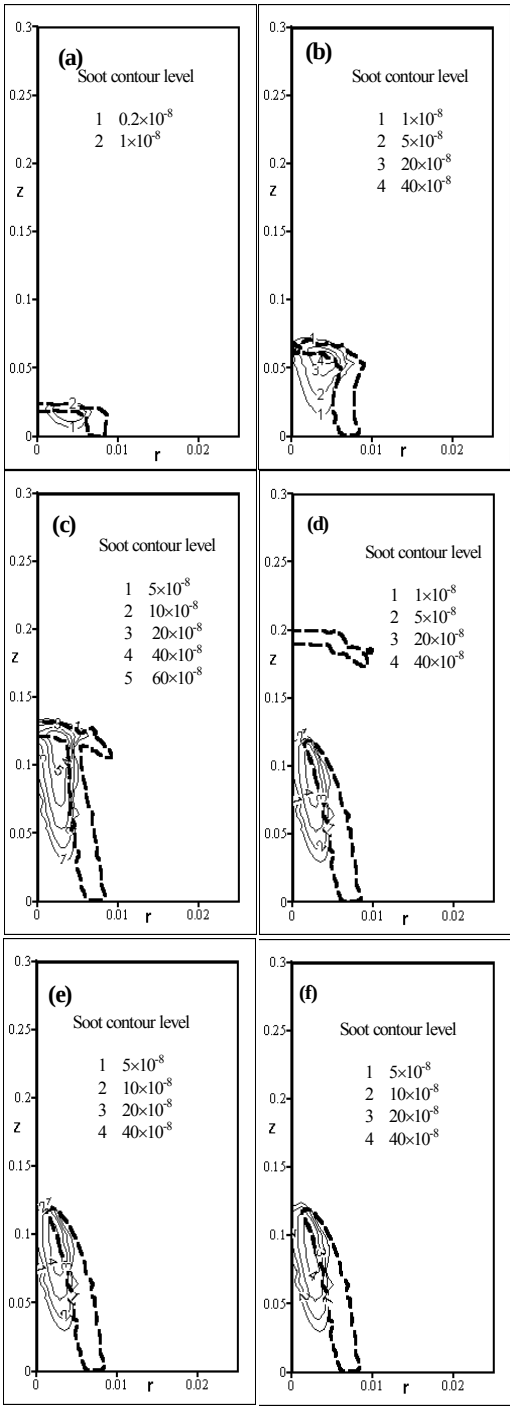

Fig.3. Flame front surface (thick dotted line) and soot volume fraction contours at different times after ignition : (a) t = 0.05 s, (b) t = 0.10 s, (c) t = 0.15 s, (d) t = 0.20 s, (e) t = 0.40 s and (f) t = 0.8 s.

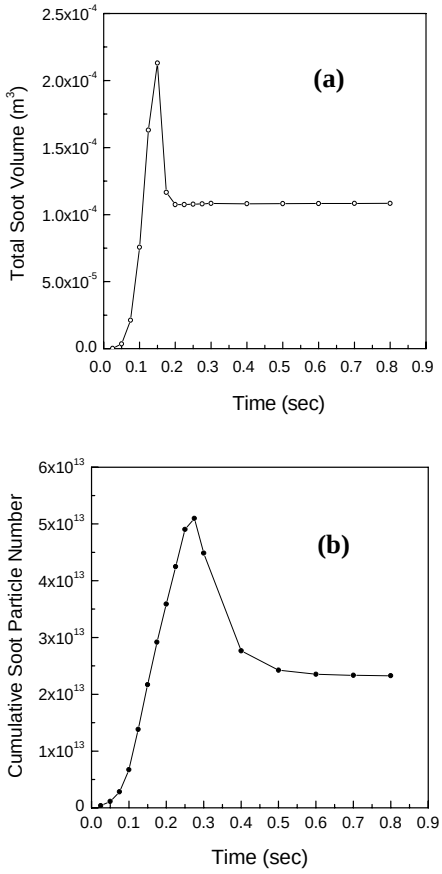

Fig 4. Variation of (a) total soot volume, (b) cumulative soot particle number with time after ignition for the diffusion flame.

In the first time zone (zone i), both nucleation and surface growth of the soot are important. However, results from the figures 4a and 4b reveal that the rate of increase of soot volume is greater than that of the particle number. This indicates that surface growth, and not nucleation, contributes significantly towards the soot formation process during the early period. This is rightly so because the activation temperature for the surface growth process ($T_\gamma = 12.6\times10^3$ K) is lower than that of soot nucleation ($T_\alpha = 46.1\times10^3$ K). As the temperature increases, the rate of nucleation increases more rapidly compared to the increase in the rate of surface growth. After 0.15 s, a high temperature is found and soot oxidation takes a very important role. Though the number of soot particles increases due to further nucleation, but oxidation overcomes the surface growth to cause a decrease in the total soot volume (zone ii). The soot surface growth is a function of the aerosol area and with the formation of more soot particles, surface growth rate increases. It finally equals the soot oxidation rate and soot volume reaches a steady value (zone iii). When

many soot particles are formed in the domain, coagulation plays a major part. This is because coagulation is directly proportional to the square of the soot number density. Coagulation does not change the soot volume in the domain but reduces the number of particles within it (zone iv). Finally, all the processes attain a state such that both the total soot volume and aggregate soot particle number reach their steady values.

The average soot particle diameter in the domain is calculated from the local values of soot volume fraction and number density as,

$$d_S = \left(\frac{6\, f_V}{\pi\, n} \right)^{0.33} \qquad (4)$$

The distributions of the average soot particle diameters in the solution domain at different times are plotted in figures 5a-f.

The maximum soot particle diameter, at steady condition is obtained as 10 nm. Figure 5a shows that initially (t = 0.05 s) the maximum soot particle size is about 4 nm, which is less than half that of the maximum size in the steady flame. The maximum soot particle size at t = 0.1 s is 10 nm (Fig. 5b) and the maximum soot size occurs within the flame. At this time the peak temperature has already increased to above 2000 K. It augments the soot formation kinetics, particularly the growth. The post flame oxidation is not so strong at this time, as the temperature did not rise sufficiently in the oxygen rich post-flame zone to accelerate the oxidation reaction. The average soot diameter at the exit plane is 2 nm, which is about one-fifth of the maximum soot particle size observed at the steady state. This clearly reveals that following ignition, before the flame completely gets stabilized, some soot particles of small size leave into the atmosphere. The situation further worsens at 0.15 s after ignition, when soot particle size leaving into the atmosphere grows to about 8 nm (Fig. 5c), which is almost equal to the peak soot size of the steady flame obtained in the present prediction. Subsequently the gases in the post flame region get heated, which increases the rate of soot oxidation beyond the flame. In the figure 5d it can be seen that 0.2 s after ignition, the gas above the flame becomes sufficiently hot to oxidize the soot just above the flame. However, the soot particles near the exit plane still remain of considerable size and escape into the atmosphere. Therefore, it is clear that immediately after ignition of a diffusion flame in a confined burner, for some length of time soot particles will escape into the atmosphere causing pollution. Subsequently, the oxidation process will consume the soot particles above the flame zone. The soot particles then get restricted within the flame zone only (figures 5e and 5f) for the present operating conditions and fuel.

5. CONCLUSIONS

A numerical investigation of soot formation under early transient condition following ignition in a laminar methane/air diffusion flame has been carried out. Predictions are tested against published data and a good agreement is obtained. It is observed that soot concentration remains pretty low initially after ignition due to low temperature. However, soot concentration in the zone increases as the temperature in the computation zone increases with time. The soot volume and the soot particle number subsequently reach their peak values, then decrease due to oxidation and coagulation of soot particles and finally attain steady values. Initially some of soot particles of small diameters leave the solution domain, but under steady state the product gas escapes with no soot.

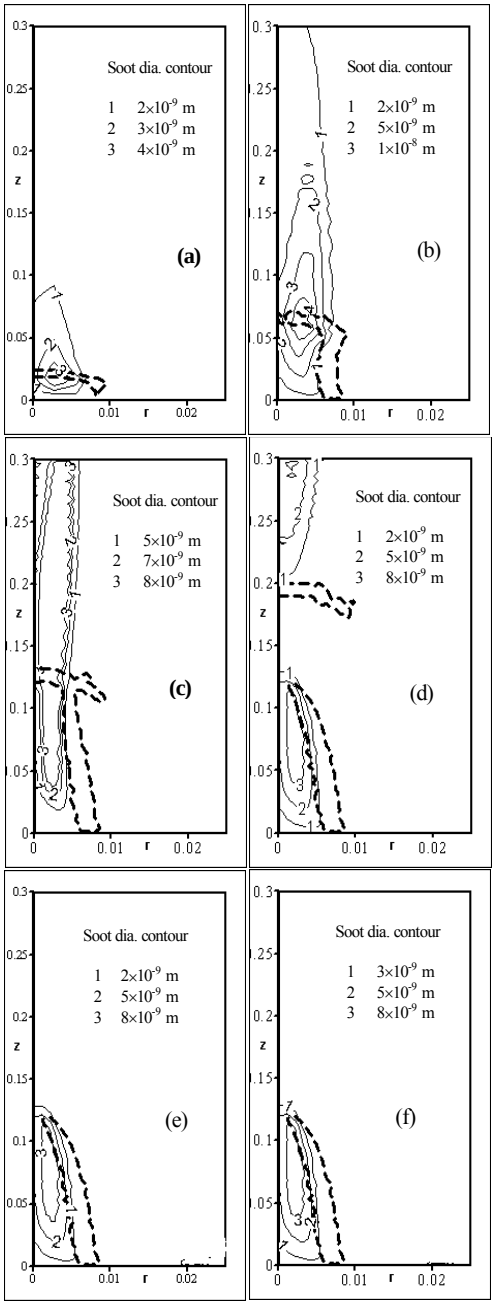

Fig 5. Flame front surface (dotted thick line) and soot diameters contours at different times after ignition: (a) t = 0.025, (b) t = 0.10 s, (c) t = 0.015 s, (d) t = 0.20 s, (e) t = 0.4 s, 9f) t = 0.8 s

6. REFERENCES

1. Haynes, B.S., Wagner, H.G., 1981, "Soot Formation", Progress in Energy and Combustion Science, 13 : 303 - 310.
2. Wey, C., Powell, E.A. and Jagoda, J.I., 1984, "The Effect of Temperature on the Sooting Behaviour of Laminar Diffusion Flames", Combustion Science and Technology, 41: 173-190.
3. Santoro, R. J., Yeh, T. T., Horvath, J.J. and Semerjian, H.G., 1987, "The Transport and Growth of Soot Particles in Laminar Diffusion Flames", Combustion and Flame, 53: 89 -115.
4. Smooke, M.D., McEnally, C.S., Pfefferle, L.D., Hall, R.J., and Colket, M.B., 1999, "Computational and Experimental Study of Soot Formation in a Coflow, Laminar Diffusion Flame", Combustion and Flame, 117 : 117 -139.
5. Lee, K. O., Megaridis, C.M., Zelepouga, S., Saveliev, A. V., Kennedy, L.A., Charon, O. and Ammouri, F., 2000, "Soot Formation Effects of Oxygen Concentration in the Oxidizer Stream of Laminar Co-annular Non-premixed Methane/Air Flames", Combustion and Flame, 121 : 323 - 333.
6. Xu, F., El-Leathy, A.M., Kin, C.H. and Faeth, G.M., 2003, "Soot Surface Oxidation in Hydrocarbon/Air Diffusion Flames at Atmospheric Pressure", Combustion and Flame, 132 : 43 - 57.
7. Smith, G.W., 1982, "A Simple Nucleation/Depletion Model for the Spherule Size of Particulate Carbon", Combustion and Flame, 48 : 265 - 272.
8. Gore, J.P. and Faeth, G.M., 1986, *Twenty-First Symposium (International) on Combustion*, The Combustion Institute, Pittsburgh, pp. 1521 – 1531.
9. Kennedy, I. M., Kollmann, W., and Chen, J. Y., 1990, "A Model for the Soot Formation in Laminar Diffusion Flame", Combustion and Flame, 81 : 73-85.
10. Syed, K.J., Stewart, C.D. and Moss, J.B., 1990, "Modelling Soot Formation and Thermal Radiation in Buoyant Turbulent Diffusion Flames," *Twenty-Third Symposium (International) on Combustion*, The Combustion Institute, Pittsburgh, pp. 1533 - 1539.
11. Moss, J.B., Stewart, C.D. and Young, K.J., 1995, "Modelling Soot Formation and Burnout in a High Temperature Laminar Diffusion Flame Burning under Oxygen-Enriched Conditions", Combustion and Flame, 101: 491 - 500.
12. Said, R., Garo, A. and Borghi, R., 1997, "Soot Formation Modeling for Turbulent Flames", Combustion and Flame, 108 : 71 - 86.
13. Lee, K.B., Thring, M.W. and Beer, J.M., 1962, "On the Rate of Combustion of Soot in a Laminar Soot Flame", Combustion and Flame, 6 : 137 - 145.
14. Nagle, J. and Strickland-Constable, R.F.,1962, *Proc. Fifth Carbon Conf.*, Pergamon (Oxford), pp. 154-164.
15. Najjar, Y.S.H., and Goodger E. M., 1981, "Soot Oxidation in Gas Turbines using Heavy Fuels.2", Fuel, 60 : 987 - 990.
16. Datta, A., 2004, "Effects of Variable Property Formulation on the Prediction of a CH_4-Air Laminar Jet Diffusion Flame," *Proc.of 6th ISHMT/ASME Heat and Mass Transfer Conference*, India, pp. 532 - 540.
17. Mandal, B.K., Datta, A. and Sarkar, A., 2005, "Transient Development of Methane-Air Diffusion Flame in a Confined Geometry with and without Air-Preheat", International Journal of Energy Research, 29 : 145 - 176.
18. Heywood, J.B., 1989, "*Internal Combustion Engine Fundamentals*," Second Edition, McGraw-Hill, N.Y., U.S.A.
19. Mitchell, R.E., Sarofim, A.F. and Clomburg, L.A., 1980, "Experimental and Numerical Investigation of Confined Laminar Diffusion Flames," Combustion and Flame", 37 : 227-244.

7. NOMENCLATURE

Symbol	Meaning	Unit
d_s	Soot diameter	m^3
H_F	Flame height	m
f_V	Soot volume fraction	
N_0	Avogadro number	
n	Soot particle number density	m^{-3}
p	Pressure	bar
r	Radial distance	m
$\dot{S}_\varphi$	Source term in conservation equations	
T	Temperature	K
T_α	Activation temp. for soot nucleation	K
T_β	Activation temp. for soot surface growth	K
t	Time	s
v	Velocity	$m.s^{-1}$
V_t	Thermophoretic velocity	$m.s^{-1}$
z	Axial distance	m
Greek symbols		
ρ_s	Soot particle density	$kg.m^{-3}$
ω_{OX}	Soot oxidation rate	$m^{-3}.s^{-1}$
φ	General variable in conservation quations.	
Subscript		
r	Radial direction	
z	Axial direction	

8. MAILING ADDRESS

Bijan Kumar Mandal
Department of Mechanical Engineering
Bengal Engineering and Science University
Shibpur, Howrah 711 103
India
Phone: 91-033-26684219
Fax: 91-033-26684561
E-mail: bkm375@yahoo.co.in